Modeling of Proximity Effect on Positive Leader Inception and Breakdown of Long Air Gaps

Farouk A. M. Rizk, *Life Fellow, IEEE*

***Abstract*—The paper presents the first effort to mathematically model proximity effects on continuous leader inception and breakdown of long air gaps under critical switching impulses. Three aspects of proximity with considerable practical importance are addressed. These include wall proximity in high voltage switching impulse tests, effects of protrusions and surface roughness on switching impulses performance of large electrodes and finally determination of critical ground fields for upward leader inception of a vertical rod under an energized plane electrode. The model results provide quantitative tools to assess proximity effects as well as means to keep such effects within acceptable limits. Whenever possible the model findings are compared with experimental results and internationally recommended practice and with view of the complexity of the problems, the agreement is quite satisfactory.**

***Index Terms*—Air gaps, high-voltage testing, leader discharge, lightning, switching impulse.**

I. Introduction

POSITIVE leader inception is of fundamental importance to switching impulse breakdown of long air gaps as well as for the attachment process of direct lightning strokes [1]–[3]. Positive leader inception criteria for the basic configurations of rod-plane and conductor-plane gaps were formulated in [4]. The model has been successfully applied to more complex configurations, including rod-rod, conductor-rod, conductor-conductor, and conductor-tower leg [5]–[7]. It has also been successful in accounting for the effect of air density (altitude) on air-gap breakdown [8].

In many practical situations, the breakdown of long air gaps under slow front impulses is known to be influenced by the proximity of grounded or live objects [9]. These situations include:

- the effect of walls of a high-voltage test hall on the breakdown voltage of long air gaps; in fact, such an effect became the determining factor in dimensioning a high-voltage hall for ultra-high-voltage (UHV) testing [10];
- the effect of small protrusions on positive switching impulse breakdown of large electrodes-to-ground air gaps; the effect was found to be so important as to bring the breakdown voltage of a large electrode gap down to the level of the corresponding rod plane [11], [12];
- the effect of position of an upper HV plane electrode on upward positive leader inception from a grounded rod [13], simulating an upward connecting leader.

The aforementioned situations are normally dealt with empirically or by following the general IEC-60 recommendation [9] which states that "a clearance to extraneous structures not less than 1.5 times the length of the shortest possible discharge path on the test object usually makes such proximity effects negligible." No physically based mathematical model has been previously formulated to deal with the proximity effect in the situations described before. For the first time, this paper describes such an approach with the objective of quantifying the effects involved. Whenever possible, the model findings will be compared to experimental results and to the aforementioned IEC recommendation

II. Continuous Leader Inception

Contrary to a positive streamer which is characterized by a practically constant mean voltage gradient in the range of 400–500 kV/m, a leader is an arc-like discharge with a mean voltage gradient that varies within a relatively much wider range and which decreases with both leader current and time of existence [14]. The quasi-stationary leader gradient varies typically in the range 50 kV/m to 3 kV/m, and can therefore, compared to the streamer, span much longer air gaps with only moderate applied voltage demand.

Leader current is provided by streamers ahead, called leader corona, and therefore streamers constitute a prerequisite for leader formation. Conversely streamer suppression (e.g., by using large electrodes under clean and dry conditions) inhibits leader formation and enhances the dielectric withstand of an air gap.

The term "continuous leader" refers to a leader which once initiated, would continue to cross the air gap, while a leader which stops after bridging a limited distance is referred to as an aborted leader.

In [5], two criteria were formulated for the continuous positive leader onset:

- formation of a stem at the streamer root, which is associated with the injection of a critical charge associated with a critical streamer size characterized by the ratio between the streamer charge Q_o and the applied voltage U; this ratio has the dimension of capacitance;
- for continuous propagation, the net electric field at the leader tip must exceed a critical value; the net electric field referred to here is the result of the applied electric field and the opposing space charge fields due to leader corona and due to its image charge on the ground electrode.

Manuscript received October 16, 2008; revised March 03, 2009. Current version published September 23, 2009. Paper no. TPWRD-00734-2008.

The author is with Expodev, Inc. and Lightning Electrotechnologies, Inc., Montreal, QC H3B 3K9, Canada.

Digital Object Identifier 10.1109/TPWRD.2009.2027494

In [4], two basic air gaps were investigated: 1) a rod plane and 2) conductor plane. These two configurations are fundamentally different as far as discharge formation is concerned because the electric field in the vicinity of the high-voltage electrode is basically spherical for the rod electrode and cylindrical for the conductor. For a rod-plane gap, the expression for the minimum continuous leader inception voltage for a switching impulse voltage with a critical front [5] was derived as

$$\mathrm{U_{lc}} = \frac{1556}{1 + \frac{3.89}{\mathrm{h}}} \quad (\mathrm{kV, m}) \tag{1}$$

where h is the gap distance in meters. Expression (1) is independent of the size of the rod (sphere) electrode as long as

$$\mathrm{U_{lc}} > \mathrm{U_{ci}} \tag{2}$$

where $\mathrm{U_{ci}}$ is the corona onset voltage for the electrode concerned. If

$$\mathrm{U_{lc}} = \mathrm{U_{ci}} \tag{3}$$

the electrode radius is often referred to as the critical radius $\mathrm{r_c}$. As mentioned before for $\mathrm{r} < \mathrm{r_c}$, the continuous leader inception voltage is independent of the electrode radius, while for $\mathrm{r} > \mathrm{r_c}$, the corona inception voltage and continuous leader inception voltage coincide. Note that the critical radius is not a constant but increases with the gap length h. However, as the continuous leader inception voltage $\mathrm{U_{lc}}$ saturates at very large values of h in (1), the critical radius $\mathrm{r_c}$ also saturates.

For the conductor-plane gap, the expression for the minimum required continuous leader inception voltage for a switching impulse with a critical front [5] was derived as

$$\mathrm{U_{lc}} = \frac{2247}{1 + \frac{5.15 - 5.49 \ln \mathrm{a}}{\mathrm{h} \cdot \ln \frac{2\mathrm{h}}{\mathrm{a}}}} \quad (\mathrm{kV, m}) \tag{4}$$

where a is the conductor radius in meters and h, as before, is the conductor height above ground. More generally, the continuous leader inception voltage can be expressed as [5]

$$\mathrm{U_{lc}} = \frac{\mathrm{U_{c\infty}}}{1 + \frac{\mathrm{A}}{\mathrm{R}}} \tag{5}$$

where $\mathrm{U_{c\infty}}$ is a constant corresponding to the value of $\mathrm{U_{lc}}$ for very large gaps as clear from (1) and (4). A is a constant for a rod (sphere)-type electrode and varies slightly with the conductor radius for a conductor-type gap. R is a function of the electrode and gap geometry, particularly the gap spacing, and for an arbitrary geometry, [13] can be determined by using the charge simulation method [15].

The model, which obviously constitutes a physical approach, has been extensively tested against experimental results with extremely satisfactory results [5]–[7]. It may be worth mentioning that in discussing [4], Prof G. Carrara stated [16] that the success of a physical approach should be based on: 1) the number of *constant* parameters necessary to calculate the discharge voltages of a given number of insulation configurations; 2) whether these parameters are based on physical aspects of the discharge; and 3) the validity of the model in regions far from the results on which the parameters were evaluated. Prof. Carrara concluded [16] that in its field of application, the model meets the aforementioned three requirements much better than any similar approach presented up to that time.

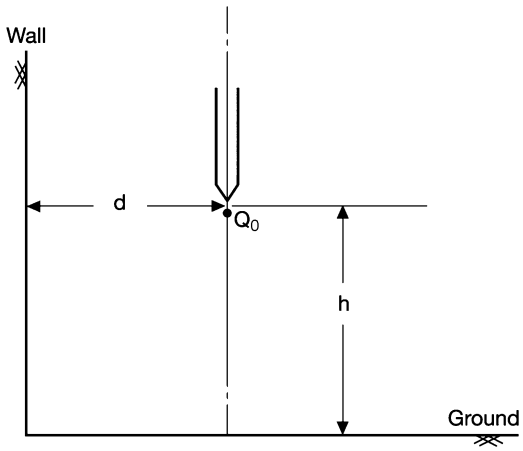

Fig. 1. Rod-plane gap with wall proximity.

Investigation of the function R either analytically of by the charge simulation method offers a powerful tool to evaluate the proximity effect on continuous leader inception for the practical situations of interest listed in the introduction before.

The function R is determined from the critical streamer space charge $\mathrm{Q_o}$ and the corresponding magnitude of the induced voltage $\mathrm{V_i}$, in the vicinity of the high-voltage electrode, due to ground images of such a charge [5]. For the simple case of a rod-plane gap with an image of $-\mathrm{Q_o}$ at a distance h below the ground plane, the magnitude of $\mathrm{V_i}$ is

$$\mathrm{V_i} = \frac{\mathrm{Q_o}}{4\pi\varepsilon_\mathrm{o}\mathrm{R}} = \frac{\mathrm{Q_o}}{4\pi\varepsilon_\mathrm{o} \cdot 2\mathrm{h}} \tag{6}$$

from which in this case $\mathrm{R} = 2\mathrm{h}$. More complex cases are treated below.

III. Rod-Plane Gap With Wall Proximity

Consider the rod-plane gap h in Fig. 1 with a wall at a lateral distance d from the gap axis.

A critical switching impulse is applied to the rod and $\mathrm{Q_o}$ refers to the steamer space charge in the rod tip vicinity. The magnitude of the voltage Vi induced in the rod vicinity (with the rod removed) due to the image charges on the ground plane and the wall will be

$$\mathrm{V_i} = \frac{\mathrm{Q_o}}{4\pi\varepsilon_\mathrm{o}} \left[\frac{1}{2\mathrm{h}} + \frac{1}{2\mathrm{d}} - \frac{1}{2\sqrt{\mathrm{h}^2 + \mathrm{d}^2}} \right] \tag{7}$$

with

$$\mathrm{V_i} = \frac{\mathrm{Q_o}}{4\pi\varepsilon_\mathrm{o}\mathrm{R}}.$$

It follows that:

$$\frac{1}{\mathrm{R}} = \frac{1}{2\mathrm{h}} + \frac{1}{2\mathrm{d}} - \frac{1}{2\sqrt{\mathrm{h}^2 + \mathrm{d}^2}} \tag{8}$$

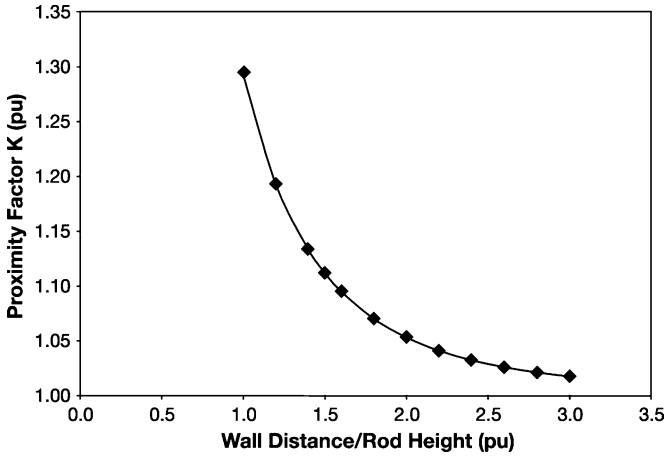

Fig. 2. Variation of wall proximity factor K with wall distance to rod height ratio.

which can be written as

$$\frac{1}{\mathrm{R}} = \frac{1}{(\mathrm{R_o}/\mathrm{K})} \tag{9}$$

where $\mathrm{R_o} = 2\mathrm{h}$, which is the value in the absence of the wall and K is a proximity factor due to the presence of the wall

$$\mathrm{K(h/d)} = 1 + \frac{\mathrm{h}}{\mathrm{d}} - \frac{\mathrm{h/d}}{\sqrt{1 + \left(\frac{\mathrm{h}}{\mathrm{d}}\right)^2}}. \tag{10}$$

Variation of the wall proximity factor according to (10) with the ratio d/h is shown in Fig. 2. The same result applies for a conductor-plane gap.

It follows that for a rod-plane gap, the general expression for the continuous leader inception voltage would be:

$$\mathrm{U_{lc}} = \frac{1556}{1 + \mathrm{K} \cdot \frac{3.89}{\mathrm{h}}} \qquad (\mathrm{kV, m}) \tag{11}$$

where K is the proximity factor expressed by (10). Similarly, for a conductor-plane gap

$$\mathrm{U_{lc}} = \frac{1556}{1 + \mathrm{K} \cdot \dfrac{5.15 - 5.49 \ln \mathrm{a}}{\mathrm{h} \cdot \ln \frac{2\mathrm{h}}{\mathrm{a}}}} \qquad (\mathrm{kV, m}). \tag{12}$$

Since the proximity factor is greater than unity, proximity will always tend to reduce the leader inception voltage. The leader continues to penetrate the gap with a sensibly constant tip potential until the leader corona front reaches the ground plane followed by what is called a "final jump" [14]. During the final jump, the leader continues to penetrate the remaining part of the gap with progressively increasing speed. The height of the final jump is given by

$$\mathrm{h_f} = \mathrm{U_{lc}}/\mathrm{E_s} \tag{13}$$

where Es is the streamer mean voltage gradient, assuming a minimum value of 400 kV/m.

For breakdown of the main gap, the leader length $\mathrm{l_z}$ at the final jump will be

$$\mathrm{l_z} = \mathrm{h} - \mathrm{h_f} \tag{14}$$

This allows the calculation of the leader voltage drop $\mathrm{U_z}$ [4]

$$\mathrm{U_z} = \mathrm{l_z} \cdot \mathrm{E_\infty} + \mathrm{x_o E_\infty} \ln \left[\frac{\mathrm{E}_i}{\mathrm{E_\infty}} - \frac{\mathrm{E}_i - \mathrm{E_\infty}}{\mathrm{E_\infty}} \mathrm{e}^{-\frac{\mathrm{l_z}}{\mathrm{x_o}}} \right] \tag{15}$$

where $\mathrm{E_\infty}$ is the quasi-stationary leader gradient normally taken for laboratory gaps in the range 30–50 kV/m. $\mathrm{x_o} = \mathrm{v} \cdot \theta$, where v is the mean leader speed, found in laboratory gaps to be around 1.5×10^4 m/s and θ a time constant taken as 50 μs. $\mathrm{E_i}$ is the initial leader gradient taken to be equal to $\mathrm{E_s}$ (i.e., 400 kV/m).

The minimum breakdown voltage $\mathrm{U_b}$ is given by [3]

$$\mathrm{U_b} = \mathrm{U_{lc}} + \mathrm{U_z}. \tag{16}$$

Considering the dispersion mostly associated with the leader's tortuous path resulting in a standard deviation (actually coefficient of variation) σ, the 50% breakdown voltage U50 is determined as [3]

$$\mathrm{U_{50}} = \frac{\mathrm{U_b}}{1 - 3\sigma}. \tag{17}$$

The percentage error due to proximity can then be determined by comparing values of $\mathrm{U_{50}}$ of a given gap with and without the presence of the wall. This will provide a tool to assess the wall proximity effect on the precision of measurement of switching impulse breakdown voltage of long air gaps as well as the difference in proximity effects between laboratories of different dimensions. Another effect, which must be avoided for safety reasons, is that under certain conditions, the wall would be struck instead of the ground plane.

Fig. 3 shows the dependence of the error in $\mathrm{U_{50}}$ due to proximity as a function of the ratio d/h for 5-m and 10-m gaps. It is shown that for d/h of 1.5, as recommended by IEC-60 [9], the proximity error is 3.25% for a 5-m gap and 1.9% for the 10-m gap, which is acceptable. It is sometimes required to determine not only the 50% breakdown voltage $\mathrm{U_{50}}$ of a long air gap but rather to establish the full breakdown probability curve up to a practical upper limit (e.g., $\mathrm{U_{50}}(1 + 3\sigma)$). In order to prevent unwanted breakdowns in the proximity gap to the wall, the following condition is imposed on the minimum breakdown voltage to the wall:

$$\mathrm{U_{bprox}} = \mathrm{U_{50test}}(1 + \mathrm{n}\sigma) \tag{18}$$

where $\mathrm{n} \geq 3$ defines the safety margin required and σ is usually taken as 0.05. What is new in this approach is that we do not treat the statistical breakdown characteristics of the two gaps as independent, but rather coupled by the continuous leader inception voltage which is determined with due consideration to the proximity effect.

Fig. 4 shows the relationship between the safety margin parameter n and the ratio d/h of a 10-m rod-plane gap. It is shown that for $\mathrm{n} = 3$, $\mathrm{d/h} \approx 2.1$, so that a distance of 21 m to the

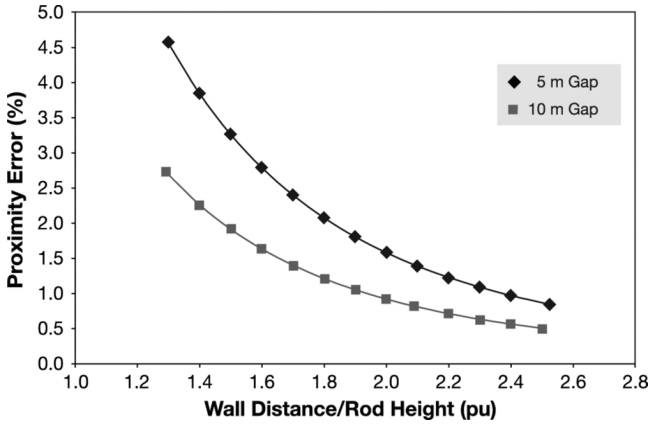

Fig. 3. Dependence of wall proximity error in U50 on wall distance to the rod height ratio under critical switching impulse.

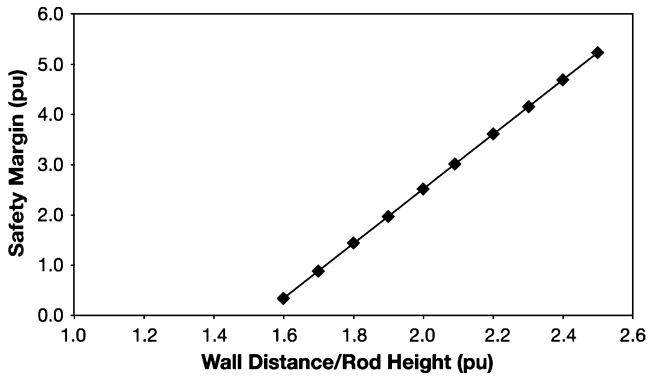

Fig. 4. Dependence of safety margin, in per unit of standard deviation, on wall distance to rod height ratio. 10-m rod-plane gap.

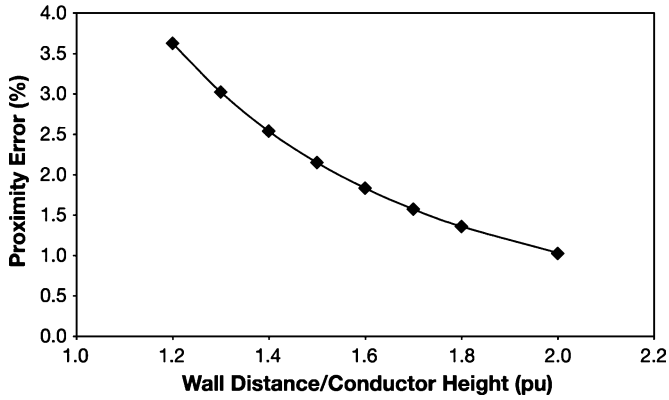

Fig. 5. Variation of the wall proximity error in U50 with the wall distance to conductor height ratio. 10-m conductor-plane gap.

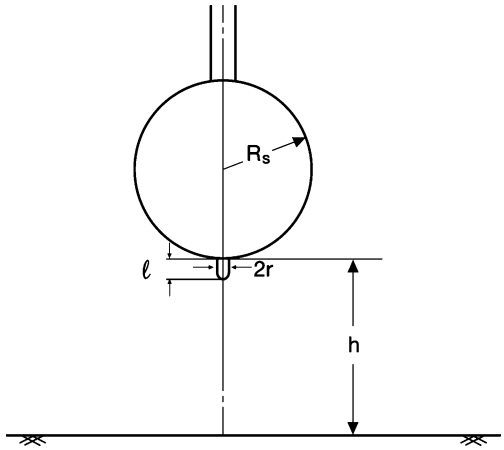

Fig. 6. Simulated protusion in a large sphere-plane gap.

wall would be required. This means that in this case, safety requirements rather than breakdown voltage measuring precision become the dimensioning factor.

IV. Conductor-Plane Gap With Wall Proximity

If the above rod is replaced by a long cylindrical horizontal conductor of radius a, the proximity factor of K(h/d) in (10) will remain the same. This would be inserted in (12) above to determine the continuous leader inception voltage. The same steps are undertaken to determine the final jump $\mathrm{h_f}$, leader length $\mathrm{l_z}$, leader voltage drop $\mathrm{U_z}$, the minimum breakdown voltage $\mathrm{U_b}$, and the 50% breakdown voltage $\mathrm{U_{50}}$, with σ taken as 0.03.

Fig. 5 shows the variation of the error due to wall proximity with d/h for a 10-m conductor-plane gap. Here, the conductor radius was taken as 2 cm. It is shown that for $\mathrm{d/h} = 1.5$, as recommended by IEC-60, the error is slightly above 2%, which is not much different from the case of the 10-m rod-plane gap for Fig. 3.

V. Effects of Protrusions on Large Electrodes

Experiments [11] have shown that the positive switching impulse breakdown voltage of a large electrode-plane gap is greatly reduced by surface protrusions, such as water drops. It was, in fact, determined that rain could bring the breakdown voltage of a sphere-plane gap down to that of the corresponding rod-plane gap.

This situation can be modeled as a small object (the protrusion) which is brought to the immediate proximity of the large electrode and is, in fact, in electrical contact with the large electrode. This experimental observation could be accounted for if it could be shown that for an applied voltage equal to the leader inception voltage of a rod-plane gap of the length concerned, the protrusion would, in fact, be in corona, thereby eliminating any advantage for the application of the large electrode under rain.

Fig. 6 shows a protrusion on a large sphere, the protrusion being simulated by a stem of length l , radius r, and a hemispherical cap. The dimensions of the protrusion are selected in the millimeter range typical of water drops in a rain test.

In order to simulate available experimental results, we consider a sphere with a radius $\mathrm{R_s} = 0.5$ m and a gap distance of 5 m. The protrusion parameters selected were $\mathrm{l} = 4$ mm and $\mathrm{r} = 2.5$ mm.

For a 5-m rod-plane gap, the model shows that the leader inception voltage amounts to 875 kV. The electric field at the protrusion tip for that voltage was determined by the charge

simulation method to be 90.8 kV/cm. Using the steamer theory, the corona inception field [17]

$$E_{ci} = 2300\left[1 + \frac{0.224}{r^{0.37}}\right] \quad (kV, m) \tag{19}$$

results in $E_{ci} = 70.2$ kV/m, which is considerably lower than the field applied.

The procedure outlined before was therefore used to determine U_{50}. The different parameters calculated by the model are $h_f = 2.19$ m, $l_z = 2.81$ m, $U_z = 218$ kV, $U_b = 1093$ kV, and, finally, $U_{50} = 1286$ kV. The measured value for the 5-m sphere-plane gap under rain as given in [11] amounts to 1284 kV. The calculations were repeated with the same protrusion for the same sphere but for a 2.5-m gap. The charge simulation showed a corona inception voltage of 639 kV, which since the leader inception voltage of the 2.5-m rod-plane gap is 608 kV, was taken as the leader inception voltage. The calculations yielded $h_f = 1.60$ m, $l_z = 0.9$ m, $U_z = 112$ kV, $U_b = 751$ kV, and finally $U_{50} = 884$ kV. The published [11] measured value amounted to 897 kV. The agreement between the model findings and experiment is quite satisfactory.

Having demonstrated the ability of the model to reproduce experimental results, it will now be appropriate for generalization of the approach. Instead of a protrusion with particular dimensions as before, let us introduce a surface roughness factor m in the corona inception field (19)

$$E_{ci} = m \cdot 2300\left[1 + \frac{0.224}{r^{0.37}}\right] \quad (kV/m, m). \tag{20}$$

For any large electrode gap of the type sphere plane, a value of m will be determined which will result in equal corona inception and continuous leader inception voltage for the corresponding rod-plane gap. This will be called the "critical surface roughness factor."

Fig. 7 shows the variation of the critical surface roughness factor m as a function of gap spacing for 1-m-diameter and 3-m-diameter spheres in the sphere-plane configuration in the range 3 m–14 m. It is shown that, in general, the critical value of m to bring the leader inception voltage of the large electrode down to that of a corresponding thin rod increases with gap spacing. This means that, in general, the longer the large-electrode gaps are, the more sensitivity there is to electrode surface roughness as compared to shorter gaps. However, the effect of gap spacing on the critical value of m is more significant for the 1-m sphere than for the 3-m sphere. The second observation is that for any gap spacing, the critical value of m is much lower for the 3-m sphere than for the 1-m sphere. This is caused by the fact that for a given rod plane gap, the leader inception voltage is fully determined by the gap length. For a fixed gap, applying this voltage to a larger sphere would necessarily reduce the electric field to which the protrusions is exposed.

VI. Critical Ground Field of Vertical Rod

Some experimental investigations have already gone into the determination of the conditions for continuous upward positive leader initiation from a vertical rod on a ground plane [13], [18]. The problem is of practical importance for lightning studies of upward flashes from tall structures due to negative cloud charge or a formation of an upward connecting leader to encounter a descending stepped negative leader.

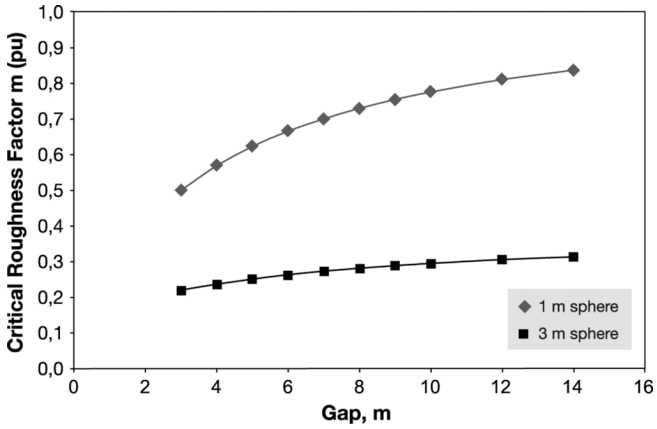

Fig. 7. Effect of sphere-plane gap on the critical surface roughness factor.

Fig. 8 shows a typical schematic representation of a test configuration, with the vertical rod placed centrally below a large electrode often energized with a negative switching impulse of several hundred microsecond front time. The leader inception is normally detected optically and/or through measurement of the discharge current at the rod ground terminal [14], [18]. Experiments can also be supplemented by electric-field measurements and/or calculations [19]. The experiment faces certain difficulties due to some usually contradictory requirements.

- In order to achieve meaningful space potential at the rod tip position for continuous leader initiation, a quasi-uniform electric field must be achieved in the plate-ground space. This requires large plate HV electrodes, and the practical characteristics of the HV voltage test sources will dictate limited gap lengths.
- Investigation of taller rods is desirable but leads necessarily to shorter gaps between the rod and the upper plane electrode, resulting in a serious proximity effect problem. Evidently in nature, no such plane exists in the vicinity of a tall structure in practical lightning considerations.

The aforementioned situation can certainly be helped by proper modeling as we intend to do below, but it is necessary to first verify that the model is capable of predicting the critical ground field for continuous leader inception in good agreement with experimental results.

Since the experimental arrangements comprise a high-voltage plane electrode and a ground plane, it is necessary to obtain an expression for the continuous leader inception voltage from a rod of height h above ground, with a distance d from the high-voltage plane as in Fig. 8.

VII. Determination of R for Two Parallel Planes

Consider a charge Q_o in the vicinity of the rod tip between two infinite planes with distances as in Fig. 8, but with the rod removed.

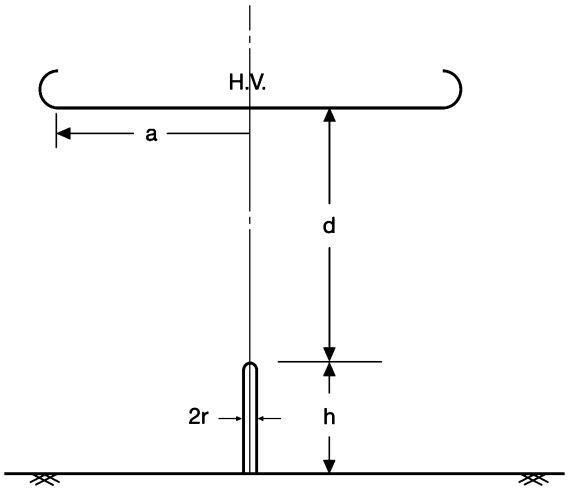

Fig. 8. Schematic diagram of test configuration to determine the critical ground field for continuous leader inception from a vertical rod on the ground plane.

Using the method of successive images, the following expression for the function R was obtained:

$$\frac{1}{\mathrm{R}} = \sum_{\mathrm{n}=1}^{\infty} \left[\frac{1}{2\mathrm{n}\cdot\mathrm{h} + 2(\mathrm{n}-1)\cdot\mathrm{d}} + \frac{1}{2\mathrm{n}\cdot\mathrm{d} + 2(\mathrm{n}-1)\cdot\mathrm{h}} - \frac{1}{\mathrm{n}\cdot\mathrm{d} + \mathrm{n}\cdot\mathrm{h}} \right] \quad (21)$$

this again can be expressed as

$$\frac{1}{\mathrm{R}} = \frac{\mathrm{K}}{\mathrm{R_o}}$$

where $\mathrm{Ro} = 2\mathrm{h}$ and $\mathrm{K} = \mathrm{K}(\mathrm{h}/\mathrm{d})$ is the proximity factor obtained from (21) for the parallel plane configuration.

Fig. 9 shows the variation of the parallel plane proximity factor with the ratio d/h. For this configuration, the space potential at the rod-tip position required for continuous leader inception will also be given by

$$\mathrm{U_{lc}} = \frac{1556}{1 + \mathrm{K}\cdot\frac{7.78}{\mathrm{R_o}}} \qquad (\mathrm{kV, m}) \quad (22)$$

where $\mathrm{R_o} = 2$ h and K is obtained from (21). From Fig. 9, it is shown that the proximity factor is very sensitive to the ratio d/h and that in order to practically eliminate the proximity effect, values of d/h as high as three may be required. The practical value of d/h, however, in any specific case will depend on the rod height h which, in turn, determines $\mathrm{R_o}$.

Consider a simulated experiment to determine the critical ground field for continuous leader inception for a grounded rod with constant height h, but with a variable gap d to the upper HV plane electrode.

In Fig. 10, h was fixed at 3.5 m, while the distance d from the rod tip to the upper plane was varied in the range 3.5–10.5 m, corresponding to inter-plane spacings in the range of 7 m–14 m. The above parameters were selected for model evaluation because of the availability of experimental results [13], [18].

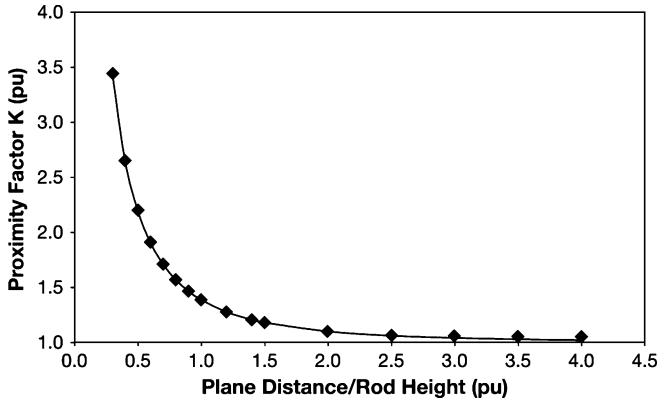

Fig. 9. Variation of parallel plane proximity factor with the plane distance to rod height ratio.

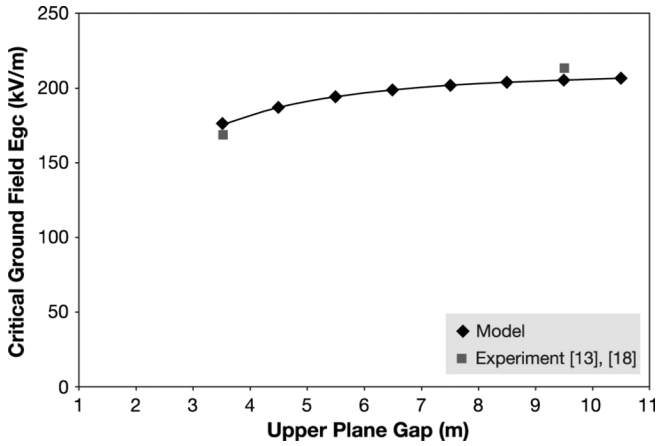

Fig. 10. Dependence of the critical ground field on the rod-upper plane gap. Rod height: 3.5 m.

It is observed in Fig. 10 that the critical ground field for the rod with a fixed height is not constant, as would be expected in free space, but increases as the distance to the upper electrode is increased, thereby reducing the proximity effect. Critical ground fields from measurements at EdF laboratory for $\mathrm{d} = 9.5$ m $(\mathrm{d/h} = 2.7)$ [18] and at CESI-ENEL for $\mathrm{d} = 3.5$ m $(\mathrm{d/h} = 1)$ [13] are also shown in Fig. 10. The results from EdF experiments amount to $\mathrm{E_{gc}}$ of 213 kV/m while the model provides a value of 205 kV/m. The CESI-ENEL measurements for the same rod height of 3.5 m resulted in a critical ground field of only 174 kV/m due to serious proximity effect, which is fully accounted for by the model results.

In another simulation, the height h of the rod was varied while maintaining the gap distance d between the rod tip and the upper infinite plane was maintained constant at 3.5 m. In this case, we calculated the critical radius of a sphere at the rod tip where the corona inception and continuous leader inception voltages coincide. Fig. 11 shows the simulation results for rod heights in the range 7 m to 24.5 m. It is observed that the critical sphere radius increases slightly despite the substantial increase in rod height. As a reference point, we include the experimental results of CESI-ENEL [13] for a 7-m rod. In the experimental point of CESI-ENEL the ratio d/h amounts to 0.5 but a test was also carried out with $\mathrm{d} = 3.5$ m and a $\mathrm{h} = 21$ m giving a d/h of 0.167.

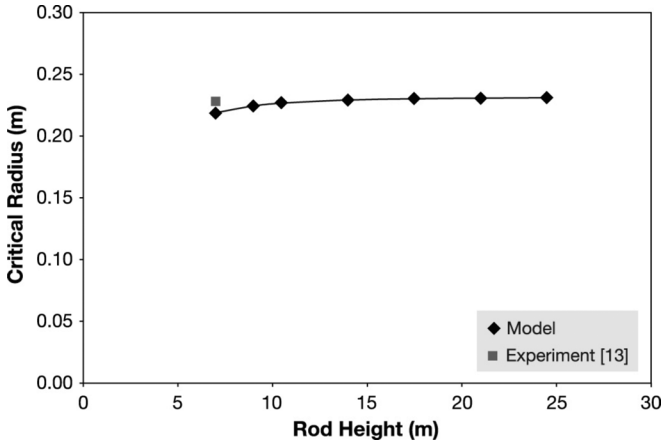

Fig. 11. Variation of critical sphere radius with rod height for 3.5-m rod-upper plane gap.

It is clear that such experiments suffer from a serious proximity effect. Reference [13] reports a critical radius of 22.5 cm for the 3.5 m/7 m test and 26.5 cm for the 3.5 m/21 m test.

According to model results, this weak dependence of the critical radius on rod height, confirmed by experimental results, is caused by the proximity effect of the upper high-voltage plane, to the extent that the measured critical radius does not belong to the rod height h but is basically determined by the distance d from the rod to the upper plane. It would therefore be erroneous to use the measured critical radius in the aforementioned experiment for a rod of the same height h in lightning conditions. The measured critical radius would simply be too low. It is worth noting that the authors of [13] observed that the measured values of the critical radius in the aforementioned experiment were much lower than those obtained in previous measurements but unfortunately they did not provide an explanation.

VIII. Determination of Critical Radius by Charge Simulation

The case of $\mathrm{d} = 3.5$ m and $\mathrm{h} = 21$ m in CESI-ENEL experiments referred to before, could not be treated analytically because the height of the upper plane (24.5 m) was large compared to the equivalent radius of the upper plane electrode, resulting in considerable electric-field nonuniformity.

We simulated the high-voltage plate by a circular disc with a radius of 10 m. Spheres of variable size supported by a 10-cm rod of variable height were also simulated. The function R was determined by charge simulation from the induced potential due to image charges on the ground and on the upper plane, at the rod-tip position, with the rod removed. Due to the limited size of the upper electrode and the large distance to ground, it was found that $\mathrm{R} = 7.45$ m, which deviates by only 6% from the value of $\mathrm{R} = 7.0$ m valid for a 3.5-m rod-plane gap. Again, this confirms that the critical ground field and the critical radius in the experiment are indeed dictated by the proximity of the upper plane electrode and not by the 21-m height of the rod.

The variation of space potential and electric field along the axis from ground to the upper plane electrode was also determined by charge simulation. As evidence of electric-field nonuniformity, the field at ground for 1000 kV at the upper electrode amounted to 22.3 kV/m, while the field at the upper plane for the same voltage reached 72.0 kV/m, with a mean electric field of 40.8 kV/m. The space potential at the rod-tip position was found to be 755.6 kV, which for a uniform field gap would have been 857 kV. The electric field at the tip of the rod was also determined by charge simulation and for 1000 kV and with a sphere radius of 24 cm came to 31.5 kV/cm. Typical simulation results are given in Table I.

TABLE I
Model Determination of Critical Sphere Radius Under the Energized Plane Electrode, d = 3.5 m, h = 21 m

r_{sph}, cm	E_{ci} kV/m	R, m	Upper Electrode Voltage		r_c, cm Exp. [13]
			V_{ci}, kV	V_{lc}, kV	
24.0	31.7	7.45	1007.5	1007.3	26.5

TABLE II
Model Determination of the Critical Sphere Radius at 21-m Height in Uniform Field Due to Cloud Charges

r_{sph}, cm	E_{ci} kV/cm	R, m	Critical Ground Field, kV/m	
			Corona Inception	Leader Inception
41.0	31.2	42.0	62.5	62.5

The results from Table I show that for a 24-cm sphere radius, the corona inception voltage and leader inception voltage are practically identical, so that the model predicts a critical radius of 24 cm. The experimental value [13] was tentatively determined at 26.5 cm. The insensitivity of the critical radius to rod height due to the proximity effect in the aforementioned experiment has been confirmed.

The question that remains to be addressed is what the critical ground field and the critical sphere radius would be in the absence of the upper plane electrode (i.e., when the space potential is created by remote cloud charges).

This situation was modeled by immersing a sphere-terminated 10-cm rod in a uniform field by charge simulation. Different sphere radii were used, keeping the sphere tip height above the ground constant at 21 m. The relevant results are given in Table II.

Based on the aforementioned results, it is concluded that the critical sphere radius for the vertical 21-m rod, in the absence of proximity effects, is 41 cm. An empirical formula based on tests at Project UHV on long air gaps [1] yields a critical radius of 37.8 cm for a 21-m gap.

IX. Conclusions

Modeling of continuous leader inception and breakdown of long air gaps under critical switching impulses has been extended to account for proximity effects. The following conclusions have been reached:

1) A proximity factor has been formulated which allows to account for the modification of the continuous leader inception by wall proximity in a switching impulse test.
2) Wall proximity manifests itself in a reduction of the continuous leader inception voltage and accordingly, the critical switching impulse breakdown voltage of a long air gap.

3) Model results provide quantitative assessment of the minimum allowable test gap-to-wall spacing in order to meet a predetermined limit for the proximity effect on breakdown voltage.
4) Model results allow the assessment of measures for the prevention of unwarranted breakdowns to the wall during switching impulse tests of long air gaps.
5) It was found that for long air gaps, safety requirements could become more stringent than the precision of the breakdown voltage in determining minimum permissible wall spacing.
6) The effect of small protrusions on continuous leader inception and critical switching impulse breakdown voltage has been addressed.
7) Protrusion effects on larger electrodes have been generalized by introducing the concept of an electrode surface roughness factor in determination of the continuous leader inception voltage.
8) It was found that for given dimensions, a large electrode leader inception voltage is generally more influenced by surface roughness the longer the air gap is concerned.
9) Otherwise, under the same conditions, a large electrode requires more severe surface roughness in order to bring down the continuous leader inception voltage to that of the corresponding thin rod.
10) The model accounted for the laboratory experiment of determining the critical ground field or critical radius of a vertical rod under an HV plane electrode, often used for the simulation of upward leaders.
11) The model demonstrated the saturation effect on the critical radius and critical ground field that could occur due to proximity of the plane electrode.
12) It has been shown that unless special precautions are taken to limit the proximity effect, the critical ground field and the critical radius will be dictated by the gap between the rod and the upper plane rather than by the rod height above ground.
13) A clear sign of the excessive proximity effect is the relative insensitivity of the critical ground field or critical radius to rod height.
14) When the proximity effect is properly limited, experimental results confirm that the mean critical ground field for continuous leader inception (stability field) is identical for vertical rods and laboratory gaps equal to rod height.
15) Comparison between model findings and experimental results has been quite satisfactory.

The model approach of assessing proximity effects described in this paper could be extended to other configurations and to outdoor installations. This is covered in a manuscript already submitted to IEEE [20]

REFERENCES

[1] L. Zaffanella, "Switching surge performance," in *EPRI AC Transmission Line Reference Book*, 3rd ed. Palo Alto, CA: EPRI, 2005, ch. 5.
[2] W. A. Chisholm and J. G. Anderson, "Lightning and grounding," in *EPRI AC Transmission Line Reference Book*, 3rd ed. Palo Alto, CA: EPRI, 2005, ch. 6.
[3] G. Carrara and L. Thione, "Switching surge strength of large air gaps: A physical approach," *IEEE Trans. Power App. Syst.*, vol. PAS-95, no. 2, pp. 512–524, Mar./Apr. 1976.
[4] F. A. M. Rizk, "A model for switching impulse leader inception and breakdown of long air gaps," *IEEE Trans. Power Del.*, vol. 4, no. 1, pp. 596–606, Jan. 1989.
[5] F. A. M. Rizk, "Switching impulse strength of air insulation: Leader inception criterion," *IEEE Trans. Power Del.*, vol. 4, no. 4, pp. 2187–2194, Oct. 1989.
[6] F. A. M. Rizk, "Critical switching impulse strength of phase-to-phase insulation," *IEEE Trans. Power Del.*, vol. 8, no. 3, pp. 1492–1506, Jul. 1993.
[7] F. A. M. Rizk, "Critical switching impulse breakdown of long bundle-conductor gaps," *IEEE Trans. Power Del.*, vol. 11, no. 1, pp. 373–383, Jan. 1996.
[8] F. A. M. Rizk, "Critical switching impulse of long air gaps: Modeling of air density effects," *IEEE Trans. Power Del.*, vol. 7, no. 3, pp. 1507–1515, Jul. 1992.
[9] *High Voltage Test Techniques*, IEC Std. 60-1, 1989, 2nd ed.
[10] N. Hylten-Cavallius and D. Train, "The IREQ ultra high voltage laboratory and test facilities," *IEEE Trans. Power App. Syst,*, vol. PAS-93, no. 1, pp. 176–186, Jan. 1974.
[11] F. A. M. Rizk, "Influence of rain on switching impulse sparkover voltage of large—Electrode air gaps," *IEEE Trans. Power App. Syst.*, vol. PAS-95, no. 4, pp. 1394–1402, Jul. 1976.
[12] C. Menemenlis, G. Harbec, and J. F. Grenon, "Switching impulse corona inception and breakdown of large high voltage electrodes in air," *IEEE Trans. Power App. Syst.*, vol. PAS-97, no. 6, pp. 2367–2374, Nov. 1978.
[13] M. Bernardi, L. Dellera, E. Garbagnati, and G. Sartorio, "Leader progression model of lightning: Updating of the model on basis of the recent test results," in *Proc. ICLP*, 1996, vol. 1, pp. 399–407.
[14] Les Renardieres group, "Research on long air gap discharges at les renardieres," *Electra*, no. 23, pp. 53–157, Jul. 1972.
[15] H. Singer, H. Steinbigler, and P. Weiss, "A charge simulation method for calculation of high voltage fields," *IEEE Trans. Power App. Syst.*, vol. PAS-93, no. 5, pp. 1660–1668, Sep. 1974.
[16] G. Carrara, "Discussion of ref. [4]," *IEEE Trans. Power Del.*, vol. 4, no. 1, p. 605, Jan. 1989.
[17] L. Thione, "The electric strength of air gap insulation," in *Surges in High Voltage Nteworks*, K. Ragaller, Ed. Baden, Switzerland: Brown Boveri, 1979, pp. 165–205.
[18] G. N. Alexandrov, G. Berger, and C. Gary, "New investigations in lightning protection of substations," presented at the CIGRE, 1994, paper no. 23/13–14, 7 pp.
[19] C. Gary and B. Hutzler, "Simulation en laboratoire de l'impact au sol (Laboratory simulation of the ground flash)," *RGE*, no. 3, pp. 20–24, 1989.
[20] F. A. M. Rizk, "Modeling of lightning exposure of buildings and massive structures," *IEEE Trans. Power Del.*, submitted for publication.

Farouk A. M. Rizk (LF'09), photograph and biography not available at the time of publication.